J|A|C|S ARTICLES

Published on Web 08/31/2009

Influence of Oxygenation on the Reactivity of Ruthenium−Thiolato Bonds in Arene Anticancer Complexes: Insights from XAS and DFT

Thamayanthy Sriskandakumar,[†] Holm Petzold,[§] Pieter C. A. Bruijnincx,[‡] Abraha Habtemariam,[‡] Peter J. Sadler,[‡] and Pierre Kennepohl*,[†]

The University of British Columbia, Department of Chemistry, Vancouver BC V6T 1Z1, Canada, University of Warwick, Department of Chemistry, Coventry CV4 7AL, United Kingdom, and University of Edinburgh, School of Chemistry, West Mains Road, Edinburgh EH9 3JJ, United Kingdom

Received May 1, 2009; E-mail: pierre@chem.ubc.ca

Abstract: Thiolate ligand oxygenation is believed to activate cytotoxic half-sandwich $[(\eta^6\text{-arene})Ru(en)(SR)]^+$ complexes toward DNA binding. We have made detailed comparisons of the nature of the Ru−S bond in the parent thiolato complexes and mono- (sulfenato) and bis- (sulfinato) oxygenated species including the influence of substituents on the sulfur and arene. Sulfur K-edge XAS indicates that S_{3p} donation into the Ru_{4d} manifold depends strongly on the oxidation state of the sulfur atom, whereas Ru K-edge data suggest little change at the metal center. DFT results are in agreement with the experimental data and allow a more detailed analysis of the electronic contributions to the Ru−S bond. Overall, the total ligand charge donation to the metal center remains essentially unchanged upon ligand oxygenation, but the origin of the donation differs markedly. In sulfenato complexes, the terminal oxo group makes a large contribution to charge donation and even small electronic changes in the thiolato complexes are amplified upon ligand oxygenation, an observation which carries direct implications for the biological activity of this family of complexes. Details of Ru−S bonding in the mono-oxygenated complexes suggest that these should be most susceptible to ligand exchange, yet only if protonation of the terminal oxo group can occur. The potential consequences of these results for biological activation are discussed.

Introduction

There is much current interest in the design of organometallic anticancer complexes[1] and, in particular, in mechanisms which selectively increase their reactivity in cancer cells. Complexes that have attracted recent interest are cytotoxic monofunctional Ru^{II} arenes. These have been shown to bind strongly to DNA[2] and induce conformational changes, including denaturation; such damage can lead to further downstream effects, for example, recognition of the adducts by specific proteins, and their repair.[3,4] Selective targeting of such complexes is crucial, and new approaches are required to expand the scope of activity of anticancer therapeutics.[4] For example, it might be possible to exploit sulfur oxidation as a mechanism for activation of Ru^{II} arene thiolate prodrugs as well as reactivation of metabolites of Ru^{II} arene anticancer drugs. In recent years it has emerged that post-translational oxygenation of cysteine thiolate (SR^-) to sulfenate (SOR^-) and sulfinate (SO_2R^-) can also play an important role in cellular regulatory processes.[5] Moreover such thiolate redox processes in proteins and enzymes are sometimes controlled by metal complexation to the S atom.[6,7] Thiolate oxygenation seems to activate cytotoxic half-sandwich $[(\eta^6\text{-arene})Ru(en)(SR)]^+$ complexes[8] toward DNA binding. Moreover SR = SG adducts with glutathione (GSH), an abundant thiol in cells, also readily undergo S oxygenation, and so redox activation may play a general role in the mechanism of action of a wide variety of these Ru^{II} arene complexes.[9,10] Herein, we show that the properties of Ru−S bonds depend on the extent of S oxygenation, on the nature of the thiolate substituent (alkyl

[†] The University of British Columbia.
[§] University of Edinburgh.
[‡] University of Warwick.

(1) Bregman, H.; Carroll, P. J.; Meggers, E. *J. Am. Chem. Soc.* **2006**, *128*, 877–884. Gras, M.; Therrien, B.; Suss-Fink, G.; Stepnicka, P.; Renfrew, A. K.; Dyson, P. J. *J. Organomet. Chem.* **2008**, *693*, 3419–3424. Nguyen, A.; Top, S.; Pigeon, P.; Vessières, A.; Hillard, E. A.; Plamont, M. A.; Huché, M.; Rigamonti, C.; Jaouen, G. *Chem.—Eur. J.* **2009**, *15*, 684–696. Novakova, O.; Nazarov, A. A.; Hartinger, C. G.; Keppler, B. K.; Brabec, V. *Biochem. Pharmacol.* **2009**, *77*, 364–374. Scolaro, C.; Bergamo, A.; Brescacin, L.; Delfino, R.; Cocchietto, M.; Laurenczy, G.; Geldbach, T. J.; Sava, G.; Dyson, P. J. *J. Med. Chem.* **2005**, *48*, 4161–4171. Yan, Y. K.; Melchart, M.; Habtemariam, A.; Sadler, P. J. *Chem. Commun.* **2005**, 4764–4776. Bruijnincx, P. C. A.; Sadler, P. J. *Curr. Opin. Chem. Biol.* **2008**, *12*, 197–206.
(2) Novakova, O.; Chen, H. M.; Vrana, O.; Rodger, A.; Sadler, P. J.; Brabec, V. *Biochemistry* **2003**, *42*, 11544–11554.
(3) Novakova, O.; Kasparkova, J.; Bursova, V.; Hofr, C.; Vojtiskova, M.; Chen, H. M.; Sadler, P. J.; Brabec, V. *Chem. Biol.* **2005**, *12*, 121–129.
(4) Ronconi, L.; Sadler, P. J. *Coord. Chem. Rev.* **2007**, *251*, 1633–1648.
(5) Charles, R. L.; Schroder, E.; May, G.; Free, P.; Gaffney, P. R. J.; Wait, R.; Begum, S.; Heads, R. J.; Eaton, P. *Mol. Cell. Proteomics* **2007**, *6*, 1473–1484. Jacob, C.; Knight, I.; Winyard, P. G. *Biol. Chem.* **2006**, *387*, 1385–1397.
(6) Maret, W. *Antioxid. Redox Signaling* **2006**, *8*, 1419–1441.
(7) Dey, A.; Jeffrey, S. P.; Darensbourg, M.; Hodgson, K. O.; Hedman, B.; Solomon, E. I. *Inorg. Chem.* **2007**, *46*, 4989–4996.
(8) abbreviations used in this manuscript: en = ethylenediamine, ar = arene, *p*-cym = *p*-cymene, hmb = hexamethylbenzene.

Scheme 1. Structures of $[(\eta^6\text{-ar})Ru(en)(SO_nR)]^+$ Complexes Involved in This Study[a]

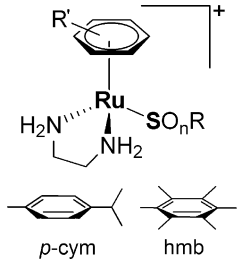

1a - n=0, R=*i*Pr, ar=*p*-cym
1b - n=0, R=*i*Pr, ar=hmb
1c - n=0, R=Ph, ar=*p*-cym

2a - n=1, R=*i*Pr, ar=*p*-cym
2b - n=1, R=*i*Pr, ar=hmb

3a - n=2, R=Ph, ar=*p*-cym
3a' - n=2, R=*i*Pr, ar=*p*-cym
3b - n=2, R=Ph, ar=hmb
3b' - n=2, R=*i*Pr, ar=hmb

[a] Complexes **3a′** and **3b′** are *in silico* models only.

or aryl), and on the arene. To make use of this ligand-centered oxidation for the design of new anticancer drugs, it is essential to understand the influence of electronic effects on the stability of the oxygenated complexes. Although the synthesis of sulfenato complexes is difficult, we recently succeeded in synthesizing a complex containing a monodentate sulfenato ligand by direct oxidation, allowing us to prepare a series of complexes with a single sulfur-containing ligand.[11] Although other studies have explored the effect of thiolato oxygenation in transition metal complexes,[7,12−15] this study is the first that allows a direct comparison of the electronic effects of a single sulfur-containing ligand and its impact on the nature of the resultant metal complexes.

Oxidation of the thiolato ligand in, e.g., complex **1** (Scheme 1) to sulfenato (**2**) and/or sulfinato (**3**) ligands plays a significant role in controlling stability and reactivity.[11] Biochemical studies suggest that ligand-centered oxidation at sulfur weakens the Ru−S bond and increases lability of the sulfur ligand, thus allowing for more facile DNA binding.[9,16,17] This observation seems incongruous with available crystallographic data, which indicate shortening of the Ru−S bond upon oxidation of the ligand (e.g., **1**→**2**),[11,14] and the short Ru−S bond in known examples of Ru^{II}−arene sulfinato complexes.[18] Furthermore, H-bonding and ancillary ligands affect the lability of the Ru−S bond implying that it is quite sensitive to such effects, although this has not been verified.[9,16,17] To explore these issues in greater detail, we have used X-ray absorption spectroscopy (XAS),[19,20] in concert with density functional theory (DFT) calculations, to probe the details of the Ru−S bond in a series of $[(\eta^6\text{-ar})Ru(en)(SO_nR)]^+$ complexes ($n = 0-2$). Recent studies have exploited such methods to investigate the biological fate of Ru^{III}-based metallodrugs.[21] Our studies show that ligand oxidation is likely to be necessary but not sufficient for biological activation of Ru^{II} arene thiolate prodrugs and that the singly-oxygenated intermediate species $[(\eta^6\text{-ar})Ru(en)(SOR)]^+$ must be protonated for ligand dissociation and DNA binding. Furthermore, specific electronic factors that contribute to observed differences in reactivity are discussed within the context of drug design.

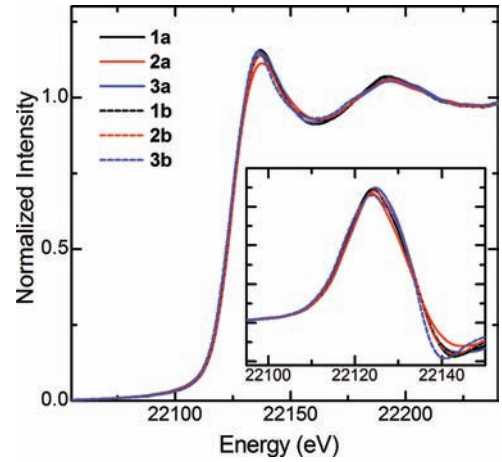

Figure 1. Normalized Ru K-edge XANES spectra of complexes of **1a,b**−**3a,b**. Inset shows the first derivative spectra indicating the edge jump position.

Results and Analysis

Solid-state Ru K-edge XAS data for thiolato (**1a**,**b**), sulfenato (**2a**,**b**), and sulfinato (**3a**,**b**) complexes are shown in Figure 1. The data are nearly superimposable in the edge region suggesting that there is no change in metal oxidation state (i.e., all complexes are Ru^{II} $4d^6$) upon ligand oxidation, thus indicating that oxygenation of the ligand does not *directly* affect the metal center. The lack of clearly observable pre-edge features in the Ru K-edge data indicates that there is little or no mixing of Ru_{5p} character into the empty $Ru_{4d\sigma^*}$ orbitals; the ligand environment is thus well described as pseudo-octahedral in all

(9) Wang, F. Y.; Weidt, S.; Xu, J. J.; Mackay, C. L.; Langridge-Smith, P. R. R.; Sadler, P. J. *J. Am. Soc. Mass Spectrom.* **2008**, *19*, 544–549.
(10) Wang, F. Y.; Xu, J. J.; Habtemariam, A.; Bella, J.; Sadler, P. J. *J. Am. Chem. Soc.* **2005**, *127*, 17734–17743.
(11) Petzold, H.; Xu, J. J.; Sadler, P. J. *Angew. Chem., Int. Ed.* **2008**, *47*, 3008–3011.
(12) Yano, T.; Wasada-Tsutsui, Y.; Arii, H.; Yamaguchi, S.; Funahashi, Y.; Ozawa, T.; Masuda, H. *Inorg. Chem.* **2007**, *46*, 10345–10353. Yano, T.; Arii, H.; Yamaguchi, S.; Funahashi, Y.; Jitsukawa, K.; Wawa, T.; Masuda, H. *Eur. J. Inorg. Chem.* **2006**, *375*, 3–3761. Rat, M.; de Sousa, R. A.; Tomas, A.; Frapart, Y.; Tuchagues, J. P.; Artaud, I. *Eur. J. Inorg. Chem.* **2003**, *75*, 9–765. O'Toole, M. G.; Kreso, M.; Kozlowski, P. M.; Mashuta, M. S.; Grapperhaus, C. A. *J. Biol. Inorg. Chem.* **2008**, *13*, 1219–1230. Mascharak, P. K. *Coord. Chem. Rev.* **2002**, *225*, 201–214. Lee, C. M.; Hsieh, C. H.; Dutta, A.; Lee, G. H.; Liaw, W. F. *J. Am. Chem. Soc.* **2003**, *125*, 11492–11493. Kung, I.; Schweitzer, D.; Shearer, J.; Taylor, W. D.; Jackson, H. L.; Lovell, S.; Kovacs, J. A. *J. Am. Chem. Soc.* **2000**, *122*, 8299–8300. Grapperhaus, C. A.; Mullins, C. S.; Kozlowski, P. M.; Mashuta, M. S. *Inorg. Chem.* **2004**, *43*, 2859–2866. Bourles, E.; de Sousa, R. A.; Galardon, E.; Giorgi, M.; Artaud, I. *Angew. Chem., Int. Ed.* **2005**, *44*, 6162–6165. Begum, F. A.; Farah, A. A.; Hunter, H. N.; Lever, A. B. P. *Inorg. Chem.* **2009**, *48*, 2018–2027. Rose, M. J.; Betterley, N. M.; Mascharak, P. K. *J. Am. Chem. Soc.* **2009**, *131*, 8340–8341. de Sousa, R. A.; Artaud, I. *Tetrahedron* **2008**, *64*, 2198–2206. Hopmann, K. H.; Himo, F. *Eur. J. Inorg. Chem.* **2008**, 1406–1412.
(13) Lugo-Mas, P.; Dey, A.; Xu, L.; Davin, S. D.; Benedict, J.; Kaminsky, W.; Hodgson, K. O.; Hedman, B.; Solomon, E. I.; Kovacs, J. A. *J. Am. Chem. Soc.* **2006**, *128*, 11211–11221.
(14) Heinrich, L.; Mary-Verla, A.; Li, Y.; Vaissermann, J.; Chottard, J. C. *Eur. J. Inorg. Chem.* **2001**, *220*, 3–2206.
(15) Dey, A.; Chow, M.; Taniguchi, K.; Lugo-Mas, P.; Davin, S.; Maeda, M.; Kovacs, J. A.; Odaka, M.; Hodgson, K. O.; Hedman, B.; Solomon, E. I. *J. Am. Chem. Soc.* **2006**, *128*, 533–541.
(16) Petzold, H.; Sadler, P. J. *Chem. Commun.* **2008**, *37*, 4413–4415.
(17) Wang, F. Y.; Habtemariam, A.; van der Geer, E. P. L.; Fernandez, R.; Melchart, M.; Deeth, R. J.; Aird, R.; Guichard, S.; Fabbiani, F. P. A.; Lozano-Casal, P.; Oswald, I. D. H.; Jodrell, D. I.; Parsons, S.; Sadler, P. J. *Proc. Natl. Acad. Sci. U.S.A.* **2005**, *102*, 18269–18274.
(18) Lindsay, C.; Cesarotti, E.; Adams, H.; Bailey, N. A.; White, C. *Organometallics* **1990**, *9*, 2594–2602.
(19) Pickering, T. J.; Prince, R. C.; Divers, T.; George, G. N. *FEBS Lett.* **1998**, *441*, 11–14.
(20) Solomon, E. I.; Hedman, B.; Hodgson, K. O.; Dey, A.; Szilagyi, R. K. *Coord. Chem. Rev.* **2005**, *249*, 97–129. Williams, K. R.; Hedman, B.; Hodgson, K. O.; Solomon, E. I. *Inorg. Chim. Acta* **1997**, *263*, 315–321.
(21) Ascone, I.; Messori, L.; Casini, A.; Gabbiani, C.; Balerna, A.; Dell'Unto, F.; Castellano, A. C. *Inorg. Chem.* **2008**, *47*, 8629–8634. Harris, T. V.; Szilagyi, R. K.; McFarlane Holman, K. L. *J. Biol. Inorg. Chem.* **2009**, *14*, 891–898.

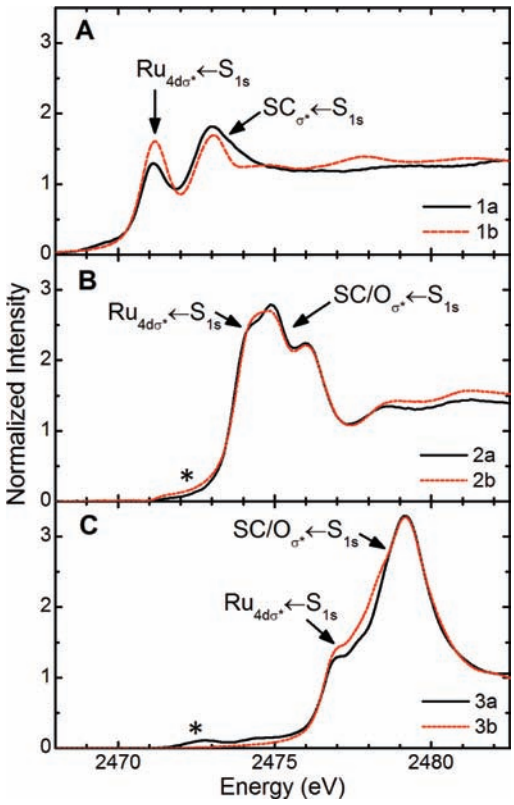

Figure 2. S K-edge spectra of Ru^{II} arene (A) thiolato **1a** and **1b**, (B) sulfenato **2a** and **2b**, and (C) sulfinato **3a** and **3b** complexes. An asterisk (*) represents features due to thiolato-based impurities in the sulfenato/sulfinato complexes (<5%).

cases.[22] Taken together, these factors confirm that ligand oxidation causes only minor perturbations at the metal center.

The S K-edge XAS spectra of these same complexes, however, differ markedly as a function of the nature of the sulfur-containing ligand as observed in Figure 2. Ligand oxidation corresponds with an overall shift of the observed transitions to higher energy by ~3 eV from **1**→**2** and from **2**→**3**, resulting from a decrease of the S_{1s} orbital energy with increasing Z_{eff}. In each of the complexes, the lowest energy feature corresponds to a $Ru_{4d\sigma^*}\leftarrow S_{1s}$ transition. The intensity of the transition derives from the electric dipole-allowed character of the atomic $S_{3p}\leftarrow S_{1s}$ transition; the intensity therefore reflects the amount of S_{3p} character in the $Ru_{4d\sigma^*}$ acceptor orbital (β) as shown in eq 1a. Given that the transition originates from a localized core orbital, contributions from other atomic orbitals (i.e., α, χ_i in eq 1a) do not significantly impact the total intensity of intense transitions.[20,23]

$$|Ru_{4d_{\sigma^*}}\rangle = \alpha|Ru_{4d}\rangle - \beta|S_{3p}\rangle - \sum_i \chi_i|L_i\rangle \qquad (1a)$$

$$I_{Ru_{4d_{\sigma^*}}\leftarrow S_{1s}} = \beta^2\langle S_{3p}|r|S_{1s}\rangle \qquad (1b)$$

For each complex, systematic peak fitting[24] and assignment of the observed spectroscopic features were performed (see Supporting Information S1). Contributions of the experimental S_{3p} to the $Ru_{4d\sigma^*}$ were estimated using the following values for the dipole integral ($\langle S_{3p}|r|S_{1s}\rangle$ in eq 1b): $\langle SR^-{}_{3p}|r|S_{1s}\rangle \simeq 8$,[25,26] $\langle SOR^-{}_{3p}|r|S_{1s}\rangle \simeq 13$,[27] and $\langle SO_2R^-{}_{3p}|r|S_{1s}\rangle \simeq 18$.[26,28] Results are listed in Table 1 with estimates of uncertainties in the fitting procedure. Our results indicate there is little change in the S_{3p} contributions to the $Ru_{4d\sigma^*}$ upon oxidation from **1**→**2** (e.g., **1a** vs **2a**), yet there is a significant drop in S_{3p} character in the fully oxygenated species (**3a,b**). Modifications of the arene ligand (*i.e.*, **a**, where ar = *p*-cym vs **b**, where ar = hmb) generate only minor differences in the spectroscopic data that cannot be distinguished within experimental error.

Table 1. Experimental Peak Energies and Transition Assignments and Experimentally Determined S_{3p} Character in the Acceptor Orbital as Estimated from Normalized Fit Intensities[a]

	S K-edge XAS transition		% S_{3p} in acceptor	
complex	energy (eV)	acceptor ← donor	XAS	DFT
1a	2471.2	$Ru_{4d\sigma^*}\leftarrow S_{1s}$	22.5 ± 1.5%	20
	2472.8	$SC_{\sigma^*}\leftarrow S_{1s}$	29.0 ± 2.0%	33
1b	2471.2	$Ru_{4d\sigma^*}\leftarrow S_{1s}$	24.0 ± 1.6%	19
	2473.0	$SC_{\sigma^*}\leftarrow S_{1s}$	17.1 ± 1.1%	29
1c	2471.4	$Ru_{4d\sigma^*}\leftarrow S_{1s}$	17.1 ± 1.4%	16
	2472.7	$\varphi_{\pi^*}\leftarrow S_{1s}$	11.7 ± 0.8%	8
	2473.5	$SC_{\sigma^*}\leftarrow S_{1s}$	27.1 ± 1.8%	*b*
2a	2474.2	$Ru_{4d\sigma^*}\leftarrow S_{1s}$	22.2 ± 1.2%	17
	2475.0	$SO_{\sigma^*}/SC_{\sigma^*}\leftarrow S_{1s}$	24.8 ± 1.2%	*b*
	2476.2	$SO_{\sigma^*}/SC_{\sigma^*}\leftarrow S_{1s}$	21.4 ± 1.1%	*b*
2b	2474.3	$Ru_{4d\sigma^*}\leftarrow S_{1s}$	22.8 ± 0.9%	18
	2475.1	$SO_{\sigma^*}/SC_{\sigma^*}\leftarrow S_{1s}$	17.8 ± 0.7%	*b*
	2476.2	$SO_{\sigma^*}/SC_{\sigma^*}\leftarrow S_{1s}$	20.6 ± 0.8%	*b*
3a	2477.1	$Ru_{4d\sigma^*}\leftarrow S_{1s}$	11.2 ± 1.3%	4 (6)[c]
	2478.1	$\varphi_{\pi^*}\leftarrow S_{1s}$	5.8 ± 1.0%	*b*
	2479.2	$SO_{\sigma^*}/SC_{\sigma^*}\leftarrow S_{1s}$	27.7 ± 2.9%	*b*
3b	2477.2	$Ru_{4d\sigma^*}\leftarrow S_{1s}$	13.2 ± 0.4%	7 (4)[c]
	2478.4	$\varphi_{\pi^*}\leftarrow S_{1s}$	8.8 ± 0.3%	*b*
	2479.4	$SO_{\sigma^*}/SC_{\sigma^*}\leftarrow S_{1s}$	33.2 ± 1.0%	*b*

[a] DFT-calculated S_{3p} contributions to the acceptor orbitals as determined from a Mulliken charge decomposition of the Kohn−Sham orbitals are also included for comparison. See Supporting Information S1 and S5−7 for further details. [b] Exact values in these cases cannot be extracted since S_{3p} character is dispersed over a wide energy range and multiple acceptor orbitals. [c] Values in parentheses are for **3a′** and **3b′**, where R = *i*Pr (see text).

As has been reported for iron−sulfinato complexes, contributions from the oxygen atoms in defining the overall charge donation from oxidized ligands cannot be neglected.[7,15] To explore these contributions, we have performed DFT calculations[29] on each of the complexes (see Supporting Information

(22) Westre, T. E.; Kennepohl, P.; DeWitt, J. G.; Hedman, B.; Hodgson, K. O.; Solomon, E. I. *J. Am. Chem. Soc.* **1997**, *119*, 6297–6314. Getty, K.; Delgado-Jaime, M. U.; Kennepohl, P. *Inorg. Chim. Acta* **2008**, *361*, 1059–1065.
(23) Solomon, E. I.; Gorelsky, S. I.; Dey, A. *J. Comput. Chem.* **2006**, *27*, 1415–1428.
(24) Delgado-Jaime, M. U.; Kennepohl, P. *J. Synchrotron Radiat.*, submitted. Delgado-Jaime, M. U.; Mewis, C. P.; Kennepohl, P. *J. Synchrotron Radiat.*, submitted.
(25) Shadle, S. E.; Pennerhahn, J. E.; Schugar, H. J.; Hedman, B.; Hodgson, K. O.; Solomon, E. I. *J. Am. Chem. Soc.* **1993**, *115*, 767–776.
(26) Sarangi, R.; George, S. D.; Rudd, D. J.; Szilagyi, R. K.; Ribas, X.; Rovira, C.; Almeida, M.; Hodgson, K. O.; Hedman, B.; Solomon, E. I. *J. Am. Chem. Soc.* **2007**, *129*, 2316–2326.
(27) The dipole integral value used for the sulfenato complexes was interpolated from that of the thiolato and sulfinato complexes since it has been previously shown that the relationship between the dipole integral and Zeff is effectively linear. See references 25, 26, and 28 for details.
(28) Neese, F.; Hedman, B.; Hodgson, K. O.; Solomon, E. I. *Inorg. Chem.* **1999**, *38*, 4854–4860.
(29) Baerends, E. J. et al.; ADF2007.01 ed.; SCM, Theoretical Chemistry, Vrije Universiteit: Amsterdam, The Netherlands, 2007. Fonseca Guerra, C.; Snijders, J. G.; te Velde, G.; Baerends, E. J. *Theor. Chem. Acc.* **1998**, *99*, 391. te Velde, G.; Bickelhaupt, F. M.; van Gisbergen, S. J. A.; Fonseca Guerra, C.; Baerends, E. J.; Snijders, J. G.; Ziegler, T. *J. Comput. Chem.* **2001**, *22*, 931–967.

S2 for details), allowing us to probe the nature of the Ru−S bond in greater detail. DFT-calculated geometries obtained using scalar ZORA relativistic corrections are in reasonable agreement with available crystallographic data (see Supporting Information S4):[11,30] Ru−S bond distances decrease with ligand oxygenation from **1**→**2**→**3**. The resultant valence MO descriptions are also in reasonable agreement with the overall trends observed in the XAS spectra (see Table 1 and Supporting Information S5−7). From these calculations, we observe that although S_{3p}⇒Ru_{4d} charge donation decreases upon oxidation, the overall ligand donor contributions remain essentially unchanged (20−23%, see Figure 3, blue squares) due in part to the compensatory effect of the oxygen atoms of the oxidized ligands. These results are consistent with those obtained by Solomon and co-workers on model systems for the active site of iron- and cobalt-containing nitrile hydratases.[7,13,15,31]

The effects of ligand oxidation on charge donation to the metal center are summarized in Figure 3; large effects are observed as a function of oxidation, and the observed trends are consistent for both hmb and *p*-cym families of complexes. Since fully oxidized alkylsulfinato complexes akin to **3a,b** have not as yet been isolated, this comparison includes *in silico* models **3a′** and **3b′** (where R = *i*Pr) to probe ligand oxidation exclusively. Importantly, we observe that although the overall ligand donation remains similar in all oxidation states, the origin of charge donation changes upon oxidation. In the alkylthiolato complexes, the Ru−S coordination bond is dominated by direct S_{3p}⇒Ru_{4d} charge donation. The first oxidation (**1**→**2**) has little effect on the S donation, but a new and relatively large contribution from the sulfenate oxygen emerges, which increases overall charge donation from the ligand. By contrast, the second oxidation step (**2**→**3**) results in a rather dramatic decrease in S character, which is compensated by the appearance of significant contributions from the alkyl R group. Importantly, the addition of a second terminal oxo group causes a net decrease in charge donation by each of the oxygen atoms. This effect is attributed to a loss of π character in the S−O bonds on going from the sulfenato to the sulfinato species, switching off an efficient mechanism for charge delocalization in the ligand. An important conclusion from these data is that charge donation from the terminal oxo groups is largest in **2**, implying that the sulfenato complexes should be most susceptible to chemical perturbations.

Ancillary ligand effects such as the nature of the arene ligand may also have an impact on the Ru−S bond although the effect when changing from *p*-cym to hmb is too subtle to quantify directly through the intensity of the $Ru_{4d\sigma^*}$←S_{1s} transition. Our DFT calculations predict a change of only 1% in the S_{3p} contribution to the bond, which is within the experimental error of our measurements (see Table 1). The SC_{σ^*}←S_{1s} transition, however, is predicted to be more sensitive to the nature of the arene ligand, and we do observe a marked change in the relative intensities of the $Ru_{4d\sigma^*}$←S_{1s} and SC_{σ^*}←S_{1s} transitions for **1b** (hmb) as compared to **1a** (*p*-cym) as well as a drop in the S_{3p} contribution for **1b** (see Table 1); this is consistent with greater electron donation from hmb[32] to the Ru center as compared to

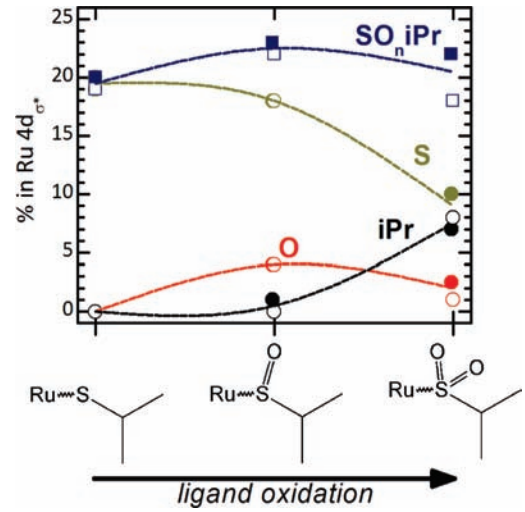

Figure 3. Breakdown of SO_nR ligand donor contributions to $Ru_{4d\sigma^*}$ orbital (in %) for **1a**→**2a**→**3a′** (filled symbols) and for **1b**→**2b**→**3b′** (open symbols) including the total ligand charge donation (blue squares) as well as specific contributions from sulfur (green circles), oxygen (per atom, red circles), and isopropyl (black circles). Lines are used to indicate general trends only.

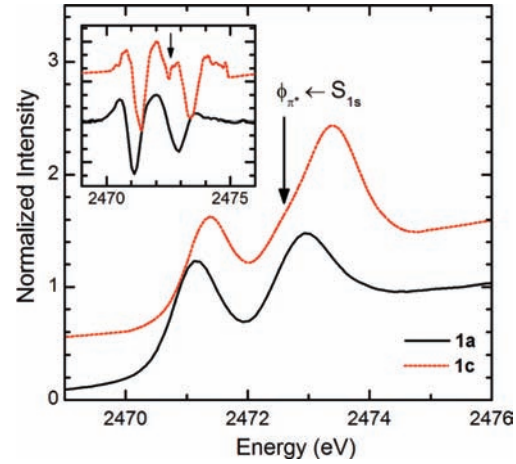

Figure 4. Normalized S K-edge XAS spectra of **1a** (black) and **1c** (red). Inset shows second derivative spectra indicating presence of a shoulder at 2472.7 eV in **1c** due to a low-lying ϕ_{π^*} orbital from the aryl moiety.

p-cym. A similar effect is also observed in the S K-edge data for the sulfenato complex (see **2a** vs **2b** in Table 1). It has previously been proposed that differences in the pK_a between **2a** (3.37) and **2b** (3.61) resulted from increased charge donation from hmb in **2b** vs *p*-cym in **2a**.[11] Our XAS data and DFT calculations are both consistent with this interpretation.

It has been observed that arylthiolato complexes of the type discussed herein are less susceptible to oxidation[16] and generally more inert than their alkylthiolato counterparts. We have therefore explored the effect of the R group in the thiolato complexes. The S K-edge XAS spectrum of the arylthiolato complex **1c** (R = Ph, see Figure 4) differs from **1a** in that a new feature appears as a low-energy shoulder on the intense SC_{σ^*}←S_{1s} feature (see Figure 4, inset). A similar feature has recently been observed in organic sulfones due to S_{3p} character mixing into aryl π* orbitals (ϕ_{π^*}) through excited state hyperconjugation.[33] The intensity of this feature therefore results from

(30) Geometries calculated without including relativistic effects or hydrogen bonding from solvent molecules (wherever appropriate based on crystallographic coordinates) tended to yield M−L bond distances that were significantly too long relative to experiment (see Supporting Information S3 for details).
(31) Kennepohl, P.; Neese, F.; Schweitzer, D.; Jackson, H. L.; Kovacs, J. A.; Solomon, E. I. *Inorg. Chem.* **2005**, *44*, 1826–1836.
(32) Govindaswamy, P.; Mozharivskyj, Y. A.; Kollipara, M. R. *Polyhedron* **2004**, *23*, 3115–3123.

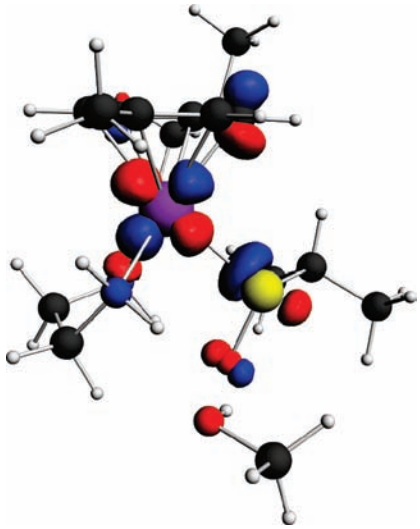

Figure 5. Graphical representation of the $Ru_{4d\sigma^*}$ Kohn−Sham orbital from **2a**.

redistribution of intensity from the main $Ru_{4d\sigma^*}$←S_{1s} transition, which must be considered when interpreting the transition intensities. From the fit intensity of the lowest energy $Ru_{4d\sigma^*}$←S_{1s} transition, the data would suggest a moderate decrease in charge donation to the metal center (from 22% to 17%, see Table 1), but the intensity redistributed through hyperconjugation (see ϕ_{π^*}←S_{1s} in Table 1) must be included. Doing so allows us to determine that the overall S_{3p}⇒Ru_{4d} charge donation is, in fact, *greater* in **1c** (∼29%) than **1a** (∼22%). The slightly increased energy of the $Ru_{4d\sigma^*}$←S_{1s} transition is also consistent with greater Ru−S covalency in **1c**. Increased charge donation from the ligand and delocalization over the aryl substituent both suggest that strengthening of the Ru−S bond and decreased susceptibility to oxidation occur for R = aryl as compared to R = alkyl.

Discussion

The combined XAS and DFT results indicate that the Ru−S bond is quite sensitive to various effects including ligand oxygenation and ancillary ligand modifications. Ru K-edge XAS data indicate that the metal center remains as a low-spin $4d^6$ Ru^{II} irrespective of the thiolato ligand oxidation state, with only minor perturbations to the overall pseudo-octahedral geometry. This is reasonable, given that the total charge donation from the S-containing ligand changes only slightly upon oxygenation, due to the compensatory effects of the terminal oxo group(s) and the R group. Sulfur oxidation therefore has very little impact on the strength and/or lability of the Ru−S bond. Importantly, S-oxygenation of the thiolato complexes to the sulfenato form changes the nature of the bond through direct involvement of the terminal oxo group. Our results further indicate that modifications to ancillary ligands (e.g., changes to the arene group) and the thiolato group have a measurable impact on the Ru−S bond.

Most importantly, our results suggest that ligand oxygenation alone is insufficient for biological activation of this family of Ru arene complexes. However, oxygenation to the sulfenato form does have an impact on reactivity through the involvement of the terminal oxo group in the metal−ligand bond as observed from inspection of the $Ru_{4d\sigma^*}$ orbital (see Figure 5). It is clearly seen that the Ru−S bond results from the interaction of one of the empty Ru 4d orbitals with the filled SO_{π^*} orbital from the sulfenato ligand. Charge donation from the SO_{π^*} orbital allows for the preservation of a highly covalent Ru−S bond even after ligand oxidation. This interaction necessarily removes electron density from the SO_{π^*} orbital, which concomitantly strengthens the S−O bond.[34,35] The nature of this orbital suggests that protonation of the terminal oxo group would directly affect Ru−S bonding. Protonation would also weaken the H-bond between the sulfenato ligand and the NH_2 of the adjacent en-ligand, an observation which is consistent with observed hydrolysis of the sulfenato complexes under acidic conditions.[11]

Based on this information, we postulate a mode of activity for the parent Ru arene thiolato complexes as depicted in Scheme 2. Oxygenation would make the prodrug susceptible to protonation at the terminal oxo group, which under acidic conditions can undergo hydrolysis and DNA binding. We note both the extracellular pH and the intracellular pH values of tumors can be acidic (pH 6−7); lysosomal compartments in cells can attain even lower pH values of 4−5.[36] In principle, even relatively low conversion to the protonated form (**2**→**2-H**$^+$) should be sufficient for activation toward ligand substitution and subsequent DNA binding. Weakening of the Ru−S bond could also occur by Lewis acid activation as has been shown in nitrile hydratase model complexes, where it has been shown that Zn^{II} binding to the terminal oxo position has a significant impact on the M−S bond.[13] In either case, activation toward ligand substitution occurs through the mono-oxygenated sulfenato form of the complex.

Knowledge of the reactivity of sulfenato and sulfinato adducts is also of importance for understanding the factors which affect the metabolism and distribution of the more general [(η^6-ar)Ru(en)(X)]$^+$ (X = Cl, Br, N_3) family of complexes, where X is generally a labile ligand. In particular, the chlorido complexes of this family have been shown to form adducts with natural thiols both outside and inside cells. The tripeptide thiol glutathione (γ-Glu-Cys-Gly), present in cells at millimolar concentrations, readily forms sulfenate and sulfinate adducts with Ru^{II} arenes,[9,10] and the blood protein albumin (ca. 0.6 mM) forms sulfinate adducts at Cys34.[37] Notably, the Ru−S bond strength is similar in **1**, **2**, and **3**, which explains why protein sulfenic and sulfinic acids[38] can compete with thiols as the preferred metal binding site in such complexes.

Conclusions

We have described herein an X-ray absorption spectroscopic and density functional theory computational analysis of the effect of arene and thiolato ligand modifications and thiolato oxygenation on the nature of the Ru−S bonds in a series of Ru arene anticancer prodrugs. Most therapeutic metal complexes are

(33) Martin-Diaconescu, V.; Kennepohl, P. *Inorg. Chem.* **2008**, *338*, 1038–1044.
(34) Goto, K.; Holler, M.; Okazaki, R. *J. Am. Chem. Soc.* **1997**, *119*, 1460–1461. Ishii, A.; Komiya, K.; Nakayama, J. *J. Am. Chem. Soc.* **1996**, *118*, 12836–12837.
(35) DFT calculations on model Cd(II)−SO*i*Pr and Ru(II)−SO*i*Pr species confirm that orbital mixing with the Ru 4d orbitals causes a decrease in the S−O bond distance. See Supporting Information S8 for details.
(36) Tannock, I. F.; Rotin, D. *Cancer Res.* **1989**, *49*, 4373–4384. Vaupel, P.; Kallinowski, F.; Okunieff, P. *Cancer Res.* **1989**, *49*, 6449–6465.
(37) Hu, W.; Luo, Q.; Ma, X.; Wu, K.; Liu, J.; Chen, Y.; Xiong, S.; Wang, J.; Sadler, P. J.; Wang, F. *Chem.−Eur. J.* **2009**, *15*, 6586–6594.
(38) Claiborne, A.; Miller, H.; Parsonage, D.; Ross, R. P. *FASEB J.* **1993**, *7*, 1483–1490. Claiborne, A.; Yeh, J. I.; Mallett, T. C.; Luba, J.; Crane, E. J.; Charrier, V.; Parsonage, D. *Biochemistry* **1999**, *38*, 15407–15416.
(39) Votyakova, T. V.; Reynolds, I. J. *Arch. Biochem. Biophys.* **2004**, *431*, 138–144.

Scheme 2. Proposed Pathway for DNA Binding by Ru^{II} Arene Thiolate $[(\eta^6\text{-ar})Ru(en)(SR)]^+$ Complexes[a]

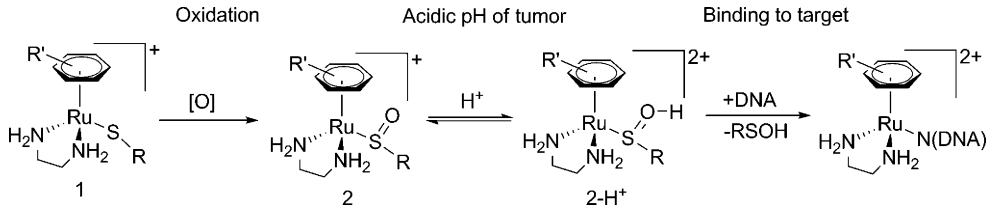

[a] The oxidation step may involve reactive oxygen species such as peroxides formed by the oxidation of GSH or NADH by oxygen.[16,39]

prodrugs; i.e. they often undergo ligand exchange or redox reactions before they reach the target site. Learning how to control such activation processes is critical to the drug design process for metallodrugs and to the construction of meaningful structure−activity relationships. In the present case the activation mechanism is rather unusual being ligand-centered, and it is important to understand how oxidation of arene−Ru−SR bonds to arene−Ru−S(O)R (sulfenate) and arene−Ru−$S(O_2)$R (sulfinate) affects reactivity.

In our studies, we have established that thiolato ligand oxygenation does not alter the charge donation to the metal center and thus should have little impact on the lability of the ligand directly. Our data therefore support the idea that additional activation is required for biological activity. An analysis of the bonding in the sulfenato species indicates that the metal−sulfur bond should be strongly affected by protonation and/or Lewis acid activation of the terminal oxo group. We further note that modifications of the parent thiolato complexes seem to be *amplified* in the oxidized complexes as evidenced by larger changes in charge donation and in the energies of the empty valence orbitals. Thus, small modifications in the parent complexes lead to major effects in the oxidized species, a finding which should be exploitable in optimizing the design of this class of anticancer complexes.

Experimental Section

Synthesis. Complexes **1** (thiolates) and **2** (sulfenates) were prepared according to previously published procedures.[11] Complexes **3** were typically prepared as follows: to a solution of thiolate **1b** $[(\eta^6\text{-hmb})Ru(en)(S\text{-Ph})]PF_6$ (20 mg, 0.035 mmol) in methanol (10 mL) was added hydrogen peroxide (10 mol equiv), and the solution was stirred for 16 h. The solvent was reduced to dryness, and the residue was washed with ether and crystallized from methanol. The complex $[(\eta^6\text{-hmb})Ru(en)(S(O)_2\text{-Ph})]PF_6$ (**3b**) was obtained as a yellow solid in 81% yield (17 mg, 0.028 mmol). ^{1}H NMR (500 MHz, DMSO-d_6): $\delta = 7.58$ (s, 5H), 5.19 (m, 2H, NH), 3.78 (m, 2H, NH), 2.59 (m, 2H), 2.32 (m, 2H), 2.02 (s, 18H); ESI-MS (MeOH): $m/z = 323$ (40%, $\{(\eta^6\text{-hmb})(en)Ru\}^+$, 465 (100%, $\{(\eta^6\text{-hmb})(en)Ru(S(O)_2\text{-Ph})\}^+$; Elemental analysis calcd for $C_{20}H_{31}N_2O_2RuS\cdot PF_6$: C, 39.41; H, 5.13; N, 4.60. Found: C, 39.70; H, 5.02; N, 4.58.

Sample Preparation. Samples for S K-edge XAS were mounted as a finely ground powder diluted (1:1) with boron nitride (BN) dusted on sulfur-free Kapton tape across the window of an Al plate. Ru K-edge XAS samples were finely ground and diluted (1:4) with BN. The resultant homogeneous, finely dispersed powders were pressed into a 0.5 mm thick Al spacer, sealed on both sides with Kapton tape.

XAS Data Collection. S K-edge XAS data were collected at beamline 6-2 and the new beamline 4-3 of the Stanford Synchrotron Radiation Laboratory (SSRL) using a modified low Z setup allowing for low temperature data acquisition under ring conditions of 3 GeV and 60−100 mA. The setup is a 54-pole wiggler beamline operating in high field (10 kG) mode with a Ni coated harmonic rejection mirror and a fully tuned Si (111) double crystal monochromator. Details of the beamline and data acquisition set are described in the literature.[40] Energy calibration of the spectra was performed using sodium thiosulfate ($Na_2S_2O_3$) with the first pre-edge feature being calibrated at 2472.02 eV. Calibration scans were performed before and after every data set to ensure stable monochromator readings. Signal was detected with a N_2 fluorescence (Lytle) detector at ambient temperature and pressure (~1 atm, 298 K).

Ru K-edge XAS data were collected at SSRL on beamline 7-3 under ring conditions 80−100 mA at 3.0 GeV. This beamline has a 20-pole, 2 T wigglers, 0.8 mrad beam, and a Si (220) double-crystal monochromator that was detuned by 50% intensity to attain harmonic rejection. The incident X-ray intensity (I0), sample absorption (I1), and Ru reference absorption (I2) were measured as transmittance using argon-filled ionization chambers. Six to eight sweeps were taken for each sample, and all data were measured to $k = 15$ Å^{-1} at 13 ± 3 K within an Oxford Instruments CF1208 continuous-flow liquid helium cryostat. Details of the experimental configuration have been described previously.[41]

Data Processing and Analysis. SIXpack was used for XAS data reduction.[42] During the process of S K-edge, pre- and post data calibration scans were compared and the energy scale of the data was adjusted by taking the first derivative of the first pre-edge feature of $Na_2S_2O_3$ being set to 2472.02 eV. Prior to normalization all the acceptable scans were averaged, fit to a linear background, and subtracted from the entire spectrum. The post-edge region was accomplished by fitting to cumulative pseudo-Voigt functions and normalized to an edge jump of 1.0. *BluePrint XAS*[24] was used to fit the pre-edge peaks by fitting the area under peaks to pseudo-Voigt functions. A Monte Carlo based method is used to simultaneously fit the background and the spectroscopic features.

The Ru K-edge XANES region was analyzed using SIXpack, and all the identical transmission sweeps for a complex were averaged and energy calibrated using Ru foil as an internal reference, with the lowest energy inflection point assigned as 22117 eV. Background subtraction and normalization were performed simultaneously using a linear pre-edge function and a quadratic post edge function.

DFT Calculations. The initial coordinates of complexes used for DFT calculations were obtained directly from the X-ray crystal structures. DFT calculations were performed using the Amsterdam Density Functional (ADF) Package Software 2007.01. Geometry optimization was followed by single-point calculations and fragment analysis. These calculations were obtained by using a BP86 (Becke−Perdew 86) gradient-corrected functional and a triple-ζ polarization (TZP) basis set with scalar ZORA relativistic correction for Ru metal unless otherwise stated. The small frozen core basis set approximation was applied with no molecular symmetry. The general numerical integration was 6.0. To help in the assignment of the transitions fragment analysis calculations were carried out on the $[(ar)Ru(en)(SO_nR)]^+$ complexes with Ru, ar (cym and hmb), en, S, O_n ($n = 0-2$), and R (*i*Pr, Ph) as the designated fragments.

(40) Kennepohl, P.; Wasinger, E. C.; George, S. D. *J. Synchrotron Rad.* **2009**, *16*, 484–488.
(41) Getty, K.; Delgado-Jaime, M. U.; Kennepohl, P. *J. Am. Chem. Soc.* **2007**, *129*, 15774–15776.
(42) Webb, S. M. *Phys. Scr.* **2005**, *T115*, 1011–1014.

Acknowledgment. This research is funded by NSERC (Canada); UBC (infrastructure), DAAD (scholarship for HP; PKZ: D/06/45748), NWO (Rubicon scholarship for PCAB); DFT performed on infrastructure funded by CFI & BCKDF through the CHORSE. We thank Anusha Karunakaran-Datt and Vlad Martin-Diaconescu for assistance during data collection and Mario Ulises Delgado-Jaime in data analysis and peak fitting. Special thanks to Dr. Serena DeBeer George at the Stanford Synchrotron Radiation Lightsource (SSRL) for technical and scientific assistance during data collection. Portions of this research were carried out at SSRL, a national user facility operated by Stanford University on behalf of the U.S. DOE-BES. The SSRL Structural Molecular Biology Program is supported by DOE, Office of Biological and Environmental Research, and by the NIH, National Center for Research Resources, Biomedical Technology Program.

Supporting Information Available: S K-edge XAS peak fits (S1), ADF input files (S2), relativistic and H-bonding effects on geometry (S3), X-ray crystallographic data (S4), molecular orbital description (S5−S7) and differences in S−O bond distance (S8). This material is available free of charge via the Internet at http://pubs.acs.org.

JA903405Z